Microvascular Research 80 (2010) 477–483

Contents lists available at ScienceDirect

Microvascular Research

journal homepage: www.elsevier.com/locate/ymvre

Regular Article

Experimental estimation of blood flow velocity through simulation of intravital microscopic imaging in micro-vessels by different image processing methods

Tzung-Chi Huang [a,*], Wen-Chen Lin [b], Chih-Chieh Wu [b], Geoffrey Zhang [c], Kang-Ping Lin [b]

[a] Department of Biomedical Imaging and Radiological Science, China Medical University, Taiwan
[b] Department of Electrical Engineering, Chung Yuan University, Taiwan
[c] Radiation Oncology, H. Lee Moffitt Cancer Center and Research Institute, Tampa, FL, USA

ARTICLE INFO

Article history:
Received 27 May 2010
Revised 18 July 2010
Accepted 19 July 2010
Available online 24 July 2010

Keywords:
Red blood cell
Blood flow
Velocity measurement
Optical flow
Micro-vessel

ABSTRACT

Quantization of red blood cell (RBC) velocity in micro-vessel is one of the techniques for dynamic observation of microvascular mechanisms. The flow measurement of RBC in micro-vessels is still a challenge nowadays. Image processing for velocity measurement using a frame by frame analysis is a common approach. The accuracy of the calculations, which is algorithm dependant, has rarely been examined. In this paper, we evaluated the accuracy of the existing methods, which includes cross correlation method, Hough transform method, and optical flow method, by applying these methods to simulated micro-vessel image sequences. Simulated experiments in various micro-vessels with random RBC motion were applied in the evaluation. The blood flow variation in the same micro-vessels with different RBC densities and velocities was considered in the simulations. The calculation accuracy of different flow patterns and vessel shapes were also examined, respectively. Based on the comparison, the use of an optical flow method, which is superior to a cross-correlation method or a Hough transform method, is proposed for measuring RBC velocity. The study indicated that the optical flow method is suitable for accurately measuring the velocity of the RBCs in small or large micro-vessels.

Introduction

The relationship between blood flow in microcirculation and the clinical physiology in blood circulation has been a wide-reaching and in-depth understanding. Various risk factors of diseases can be related to corresponding changes in microcirculation. For instance, Raynaud's syndrome(Wollersheim et al., 1988; Bertuglia et al., 1999), hypertension(Bonacci et al., 1996; Cesarone, 2000) or diabetes(Chang et al., 1997; Tibiriçá et al., 2007) are usually accompanied with impaired microcirculation. Therefore, information in blood flow of microcirculation plays an important role in health assessment and angiopathy prevention. Dynamic observation of microvascular mechanisms thus provides a deeper understanding of diseases and their relationship to the physiological function of microcirculation.

Quantization of the red blood cell (RBC) velocity in micro-vessels is a means of such observation. However, the flow measurement of RBC in micro vessels is still a challenge with current techniques. The flow in large vessels is able to be measured by using electro-magnetic blood flowmeter or ultrasonic Doppler flowmeter. Plenty useful information has been obtained on alterations in flow during physiological events and in the viscous properties of blood. A major limitation of such measurements has been their inability to relate microvascular perfusion observed within individual micro-vessels to the topographical succession of arterioles, capillaries, and venules peculiar to a given tissue.

Image processing is an alternative, non-invasive approach to achieve this goal. Several literatures have been published in RBC velocity measurement in micro-vessels using dynamic video microscopy (Bollinger et al., 1974). The measurement of the displacement of relevant patterns (RBCs or plasma gaps) between two frames and the time separating them give an estimation of the RBC velocity. But it requires the selection of a good tracking pattern which appears to be difficult in larger vessels such as venules and arterioles. Several studies have focused on the use of cross correlations for the assessment of RBC velocity (Tsukada et al., 2000; Brox and Weickert, 2002). These methods can be divided into two categories: the temporal correlation and the spatial correlation methods. Umetani et al. (1989) have used image gradient method to measure microvascular red blood cell velocity and pointed out the time-varying relationship between the blood flow velocities. Recently, Optical flow has been proposed as a quantitative method of measuring the detailed velocity distribution in micro-vessels (Sugii et al 2002, Tsukada et al., 2000). The authors have developed a particle image velocimetry (PIV) technique with improved dynamic range, spatial resolution and measurement accuracy, and also analyzed the blood velocity profile in microvessels of arterioles in rat mesentery (Sugii et al., 2002). Manjunatha and Singh (2002) also used optical flow

* Corresponding author. 91, Hsueh-Shih Road, Taichung, 404 Taiwan. Fax: +886 4 2205 4179.
E-mail address: tzungchi.huang@mail.cmu.edu.tw (T.-C. Huang).

0026-2862/$ – see front matter © 2010 Elsevier Inc. All rights reserved.
doi:10.1016/j.mvr.2010.07.007

method to measure velocity profiles of a blood flow in the multiple branching of frog mesentery employing microscopic video imaging (Manjunatha and Singh, 2002). In the literature by Kempczynski and Grzegorzewski (2008), the Hough transform technique has been adopted to estimate the velocity of RBC aggregates during sedimentation. RBC velocity was also estimated by using the Hough transform method in a simulation experiment. The results show that velocity assessment performs excellently up to 750 pixels/s. At higher velocities (>1250 pixels/s), the method fails and selects an alternative orientation that results in a large velocity error (Dobbe et al., 2008).

Generally, the blood flow velocity inside microvessels in vivo is estimated along the central line of vessels. The accuracy of calculated results, which is algorithm dependant, has rarely been examined. In this paper, the red blood cell velocities in microvessels were calculated using the three mentioned measurement methods: cross correlation method, Hough transform method, and optical flow method, through simulation of intravital microscopic imaging. The accuracy of the methods was evaluated by applying these methods to simulated microvessel image sequences, of which the RBC velocities are known. The calculation accuracy of different flow patterns and vessel shapes were also examined respectively.

Materials and methods

Image generation

In microcirculation, the capillaries lie between, or connect, the arterioles and venules. Capillaries form extensive branching networks in a vivo body, which dramatically increase the surface areas available for rapid exchange of molecules. A capillary is a thin size form of vessel. Pre-capillary is a vessel lacking complete coats, located just to the arterial side of a capillary, and is about 3–5 times in diameter. It is not much different from capillary in other respects. Pre-capillary and capillary branch off from metarteriole and terminal arteriole. The simulation images were generated based on the physical (or physiological) and anatomical characteristics of microcirculation. The capillary bed is simulated in various forms, with one of them in straight line, and another clip shaped for one RBC to pass. Branching bed of pre-capillary into capillary is also simulated. A Matlab based computer program (MathWorks, version 7. 1) was used to generate the micro-vessel image sequences.

Blood is a complicate heterogeneous liquid with its viscosity varying with shear rate. It possesses non-Newtonian characteristics. Two kinds of dynamic blood flow images were simulated in this study. One was to simulate the random motion of RBC in various shapes of blood vessels. Individual RBCs suspended in autologous plasma that have random motion were studied too in this category. The other one focused on the blood flow variation with different RBC densities. This is included in our study because the density of RBC, or hematocrit, is the most important factor in blood hydrodynamic variation. The RBC density also dominates the variation in viscosity. The higher RBC density, or the higher hemotocrit, results in higher friction between the blood layers, which causes higher viscosity. Normal hematocrit is about 50% of blood in volume. In the simulation, the RBC densities were grouped to high, medium and low levels.

Vessel size and shapes

Vessel size varies in a wide range in human anatomy. Micro vessels were generated with various sizes: (1) 1-RBC wide in diameter (Fig. 1a), (2) 2-RBCs wide in diameter (Fig. 1b) and 4-RBCs wide in diameter (Fig. 1c). Different vessel shapes were generated with the Matlab-based program in order to cover various real conditions as blood flow in micro-vessels. The RBC movement in vessels followed the velocity variation shown in Fig. 1d through e. Fig. 1f and g gives 2 examples of shapes: branching and clip (or clip-shape). These shapes

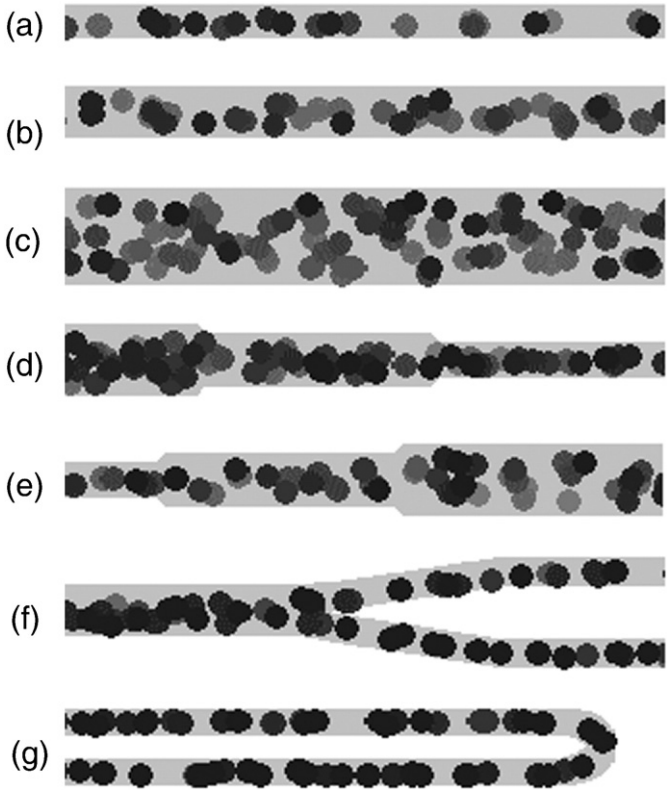

Fig. 1. Various micro-vessels. Different sizes in diameter: (a)-(c) the diameter of the micro-vessel is one, two and four times of the RBC size, respectively. (d)-(e) micro-vessel changes from narrow to wide and vice versa. (f)-(g) Two vessel shapes: (f) branching (g) clip.

can often be found in various parts of a human body. For example, the clip-shape vessel is very common in finger nail-fold.

Spatial distribution of RBC velocity in micro-vessel

The RBC velocity varies depending on the RBC location in a vessel. Mathematical expression of the RBC motion model is showing in Fig. 2. The RBC velocity V was simulated as a function of radius r inside a vessel, $V(r) = Vc(1 - r^2/R^2)$, in which Vc is the center velocity ($r = 0$), R is the vessel radius. Due to viscosity, the velocity is less in value as r increases (closer to the vessel wall). Motion in vessels of various RBC densities was also modeled. Low, medium and high density of RBC is defined based on the number of cells per unit volume. Fig. 3 shows examples of vessels with different RBC densities. With different densities, the image sequences were generated with various maximum RBC velocities of 1, 3, 5, and 10 pixels per frame respectively. The RBC velocities have a parabolic curve function in relation to the location inside a micro-vessel.

RBC velocity estimation

Cross correlation method (CCM)

Several studies have focused on the use of cross correlations for the assessment of RBC velocity (Tsukada et al., 2000). The use of these methods corresponds to the tracking of characteristic patterns in space or in time. In this study, temporal correlation was used to measure the blood flow velocity in the micro-vessels. For the temporal cross correlation methods, the transit time between two regions of the micro-vessel is estimated by measuring the intensity of two independent windows positioned on the skeleton of micro-vessel. This transit time, estimated using an image correlation function between the windows, is used to estimate the velocity.

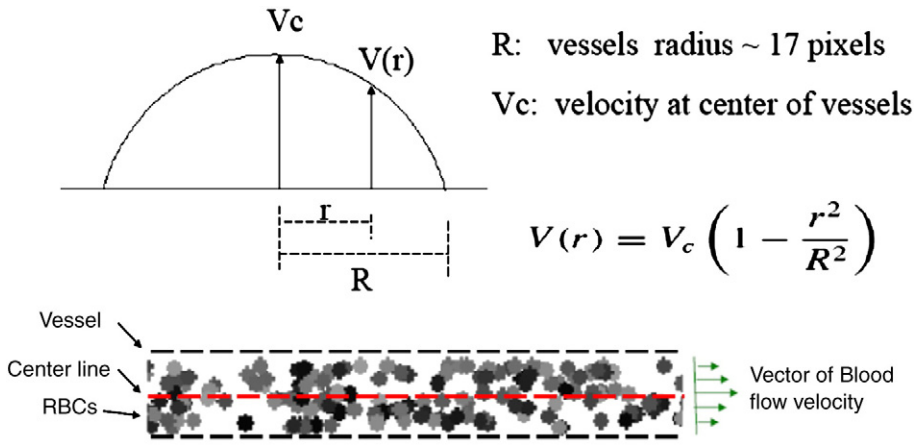

Fig. 2. The schema is to show that the RBC velocity V with the same flow direction was simulated as a function of radius r inside a micro-vessel, $V(r) = Vc(1\text{-}r^2/R^2)$, in which Vc is the center velocity ($r = 0$), R is the micro-vessel radius. Due to viscosity, the velocity is less in value as r increases (closer to the vessel wall).

In particular correlation computation, the question resolves itself into the following three points. First, skeleton extraction is applied on the image to sketch the center line (i.e., skeleton) of the vessel which is also regarded as the blood flow path in the capillary. The intensity of each skeleton pixel as in each section is determined from the images. Pixel intensity was averaged over the neighbor pixels within a 7-pixel wide square which is similar to the physical size of a RBC. Second, the maximum value of the one demotion cross-correlation between the two sequential images was calculated to obtain the frame-to-frame RBC displacement and the velocity correspondingly. Considering two series x and y where window length $i = 0, 1, 2...n$, the correlation coefficient r is defined as

$$r = \frac{S_{xy}}{\sqrt{S_{xx}S_{yy}}} = \frac{\sum_{i=1}^{n}\left[\left(x_i - \bar{x}\right) \times \left(y_i - \bar{y}\right)\right]}{\sqrt{\sum_{i=1}^{n}\left(x_i - \bar{x}\right)^2 \sum_{i=1}^{n}\left(y_i - \bar{y}\right)^2}}, \quad -1 \le r \le 1 \tag{1}$$

where $\bar{x}$ and $\bar{y}$ are the means of the corresponding series. Third, two windows with the same size were used in each site of vessel for cross-correlation computation. For two window cross-correlation, the window length was equal to a half of segment length of each site. For example, one window was located in the first half of the arteriolar limb and the other window was in the second half. Furthermore, two maximum values were obtained from these windows in each site and were averaged to present the RBC displacement in two sequential frames.

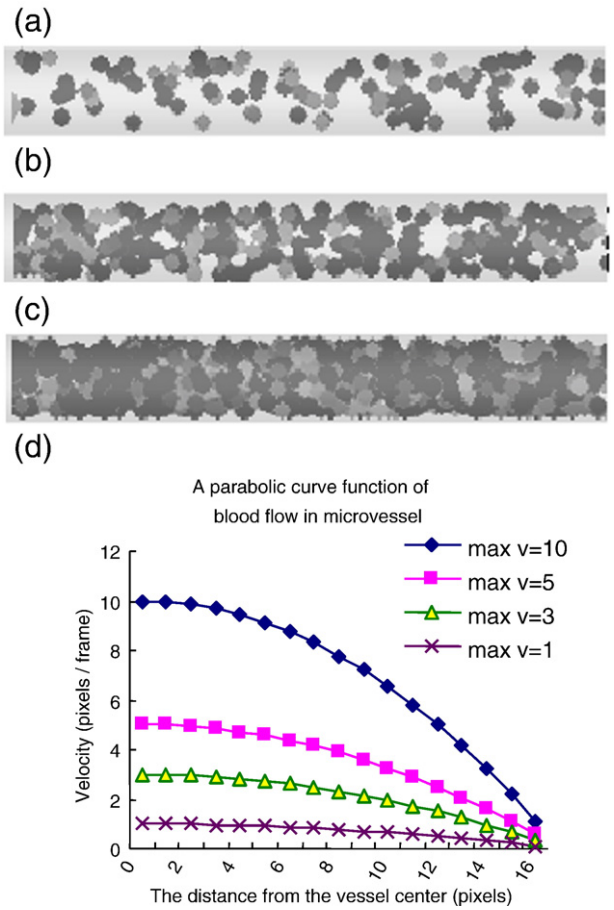

Fig. 3. An example of different RBC densities and simulated RBC velocities as functions of location in micro-vessel. In the left diagrams, low density (a), medium density (b), and high density (c) of RBCs are shown from top to bottom. The right diagram (d) indicates that RBCs in blood flow have motion with a parabolic curve function in relation to the location inside a micro-vessel.

Hough transform method (HTM)

The conventional Hough transform is a method for detecting straight lines (or curves) in images. It is basically a point-to-curve transformation that detects straight lines in images. In this study, pixel intensity of a profile image was extracted from pixels on the central line of a vessel. The intensity was averaged over the neighbor pixels within a 7-pixel wide square that is similar to the physical size of a RBC. Space-time diagram method is based on the profile image that is composed of pixel intensity on the central line of continuous frames. When the plasma gap and/or RBC in blood flow are visible, the profiles of the space-time diagram will present clear slopes for velocity determination. The horizontal axis of the space-time diagram is vessel length (distance) and the vertical axis is frame number (time). The space-time diagram was divided into small square diagrams with a size of 16×16 pixels. Slopes were automatically estimated by using Hough transform. The RBC velocity was determined by the slope of most apparently oblique line in all of the small space-time diagrams. In other words, Hough transform technique considers the polar representation of a line (Kempczynski and Grzegorzewski, 2008):

$$R = x\cos\theta + y\sin\theta \tag{2}$$

where (x, y) is the coordinate of each line pixel in the space–time diagram, θ the orientation of the vector normal to the line and starting

at the origin, and R the length of this vector, which is equal to the distance of the line to the origin. The discrete image of parameter space consists of accumulated cells, $H(\theta, R)$, that are incremented for each sinusoidal curve that passes the cell.

On a profile image, border detection is performed using the Canny edge method. Characteristic curves, straight lines in this study, are then detected using HTM. The angle θ is calculated using the straight lines. The blood flow velocity V is calculated by equation

$$V = 1 / \tan(\theta). \tag{3}$$

The horizontal axis of a profile image is the grey level distribution along the central line of a blood vessel. The spatial resolution of the image determined by hardware is 1.42 μm, and if the temporal resolution is 1/30 s, determined by the maximum sampling rate of the system. From the velocity equation

$$V = \triangle D / \triangle T, \tag{4}$$

we know that the horizontal axis of a profile image corresponds to distance while the vertical corresponds to time. As the gaps between RBCs, or the variation among the RBCs, are reflected as the grey level variation along the central axis, the characteristic lines or strips can be obtained from the profile image. Using the angle between the lines and the horizontal axis θ, the velocity equation becomes

$$V = \triangle D / \triangle T = 1 / \tan(\theta) \tag{5}$$

An example of using Hough Transform to get the angle θ from a blood flow profile image is given here. The Canny characteristic images are generated by applying Hough transform to the profile image which is shown as schema in Fig. 4a. The resulted images are shown as (b) in Fig. 4. The coordinates of the brightest spots are then located, which are the maximum values of the transform. Since the point of the longest line appears many times at the same angle, by analyzing c to f in Fig. 4, the maximum number of appearance and the corresponding angle are obtained for each image. Such brightest coordinates (R, θ) calculated for c, d, e and f are (23, −18°), (43, −19°), (40, −20°) and (26, −19°) respectively. The average blood flow velocity is thus 284.22 μm/s.

Optical flow method (OFM)

Optical flow computation results in motion direction and motion velocity at image points. The immediate aim of OFM-based image analysis is to determine a motion field. It reflects the image changes due to motion during a time interval dt, and the optical flow field is the velocity field that represents the three-dimensional motion of object points across a two-dimensional image. In the present study, this gradient-base OFM (Horn and Schunck, 1981; Wu et al., 2009; Huang et al., 2006; Zhang et al., 2008a; Guerrero et al., 2004; Zhang et al., 2008b) was applied to calculate the RBC velocity on two successive images. The velocity matrix of displacement, including horizontal and vertical movement respectively on the vessel image for each single pixel, was acquired using OFM. The velocity calculation equation in OFM is shown below.

$$v^{(n+1)} = v^{(n)} + \nabla f \left(\frac{\nabla f \cdot v^{(n)} + \frac{\partial f}{\partial t}}{\alpha^2 + \|\nabla f\|^2} \right) \tag{6}$$

where n is iteration times and $v^{(n)}$ is the average velocity derived from the surrounding pixel.

Optical flow equation calculates the difference of images and finds the deformed image to match the next frame. Originally, optical flow method (OFM) requires a very small time interval between consecutive images and no significant change occurs between two

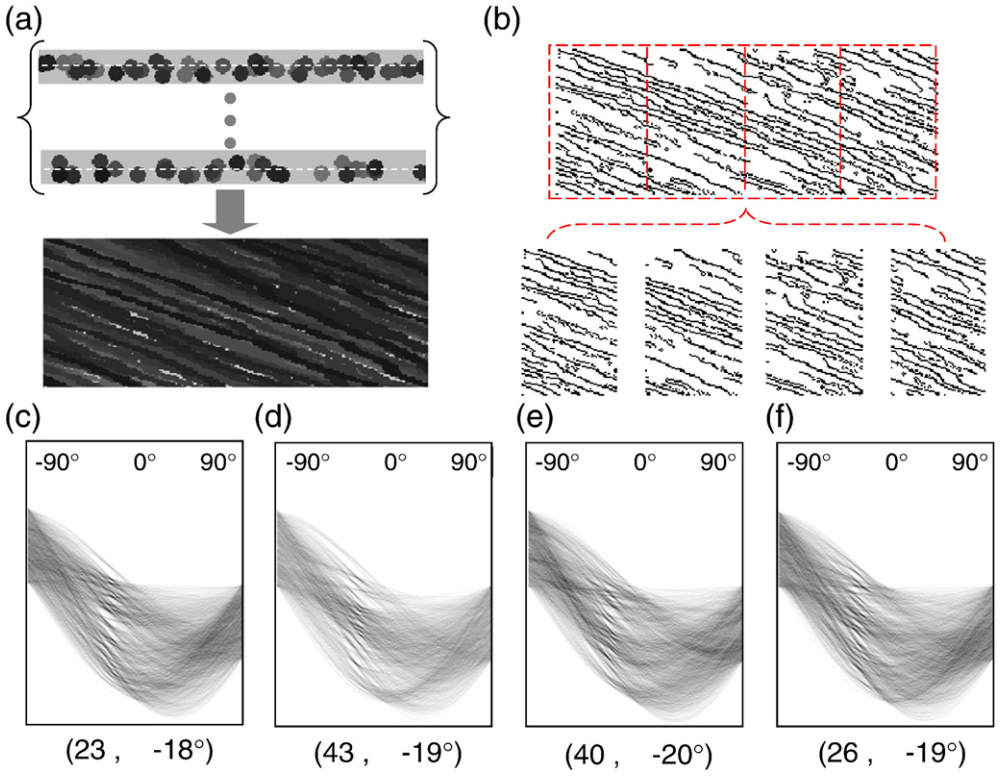

Fig. 4. (a) An image of temporal profile which was composed of intensity of pixels on the central line of micro-vessel. In this example, the length of central line is 256 pixels. (b) The edge of temporal profile (256 × 100 pixels) was obtained by using Canny edge detection, which was divided into four of small square diagrams with a size of 64 × 100 pixels from top to bottom. (c)-(f) are the Hough transformations which correspond to Canny edge detection as in (b). The angle of the maximal aggregate value of appearance for each image is (c) -18°, (d) -19°,(e) -20°and (f) -19° respectively.

Table 1
The velocity estimation in various micro-vessel cases by using three measurement methods. The vessel shape labeling is the same as it in Fig. 1.

The average error for different image processing methods, Mean ± S.D. (pixel/frame)			
Measurement			
Microvessel method shape pattern	Cross-correlation	Hough transform	Optical flow
(a)	2.693 ± 5.628	1.872 ± 0.798	0.718 ± 1.158
(b)	2.705 ± 5.619	1.958 ± 1.029	1.053 ± 1.166
(c)	2.721 ± 5.653	1.877 ± 0.986	1.115 ± 1.188
(d)	2.716 ± 5.822	2.011 ± 0.975	1.275 ± 1.166
(e)	2.704 ± 5.7107	2.043 ± 1.0931	1.070 ± 1.162
(f)	2.362 ± 4.323	2.040 ± 1.026	1.220 ± 1.171
(g)	3.288 ± 8.116	2.350 ± 0.925	1.155 ± 1.180
The overall average error of RBC displacement	2.741 ± 5.925	2.022 ± 1.001	1.087 ± 1.173

consecutive images. The original OFM developed by Horn and Schunck was not reliable in velocity calculations when object motion is significant between two consecutive frames, in which no features are overlapping.

To overcome this problem, optical flow calculations are reprocessed for a number of times with continuously updated deformed images, which converges the velocity field to accurately match the final deformation to the target image. With this implementation in the OFM, large motions can be accurately calculated and the quality of registration is significantly improved, regardless of the motion size.

Results and discussion

The velocities calculated using CCM, HTM and OFM, respectively, were compared to each other and with the known values from the simulations by the Matlab based program. This comparison was applied to various RBC densities, velocities, shapes, vessel sizes and size variations. In order to evaluate the performances of the proposed algorithms, a simulated experiment with random RBCs motion is used at first. The mean and standard deviation of differences among the calculated values in number of pixels by using the three image processing methods were listed in Table 1, which shows overall average errors of the velocity estimation in various micro-vessel cases. For the velocity estimation in various micro-vessel beds, OFM gave the minimum value in average error while CCM yielded the maximum.

According to calculations using the window diameter of 30~40 pixels for CCM, the flow velocity of the centre micro-vessel were within 2.741 ± 5.925 pixels/frame. The window size is equal to the size of sensors for CCM. The image intensity of an RBC in micro-vessels was similar to each other. This could cause uniform signal in the window, which in turn decreases accuracy significantly. For HTM, the mage of temporal profile was previously intensified by the Canny edge detection to avoid this problem. Consequently, the calculations using OFM and HTM show better agreement with known values for higher densities. The standard deviations for HTM and OFM are about 1 pixels/frame. Judging from the above, the results indicate that the OFM is a suitable image processing option.

The attention was thus focused on the evaluation of OFM in our further studies with various vessel shapes. The data analysis points were selected as shown in Fig. 5. Fig. 6a through d shows the OFM estimations of the random RBC velocities of various vessel shapes and compares them with the known values from the simulated images. The typical difference between the OFM estimations and known velocities were less than 2 pixels/frame for various micro-vessel beds.

Another experiment, which simulates the flow of RBCs in a straight line in micro-vessel with a single arteriole (diameter: 33 pixels), was generated with 50 frames. Both CCM and HTM failed and resulted with an alternative orientation and large velocity errors. Therefore, the two methods were not able to measure velocities in a larger micro-vessel, which left OFM the only choice for such cases.

The calculated velocities using OFM are compared with the known values in Table 2 and Table 3 for different RBC densities. With higher density of RBCs, more detailed structures help improving pixel-to-pixel correspondence between the images in sequence, thus better accuracy can be achieved in OFM calculations. For the low density cases, the relatively larger areas of non-cell regions in the images weaken the correspondence, which introduces larger errors in optical flow calculations. As shown in diagram a of Fig. 7, the average velocity error is less than 0.3 pixels/frame for all densities studied with

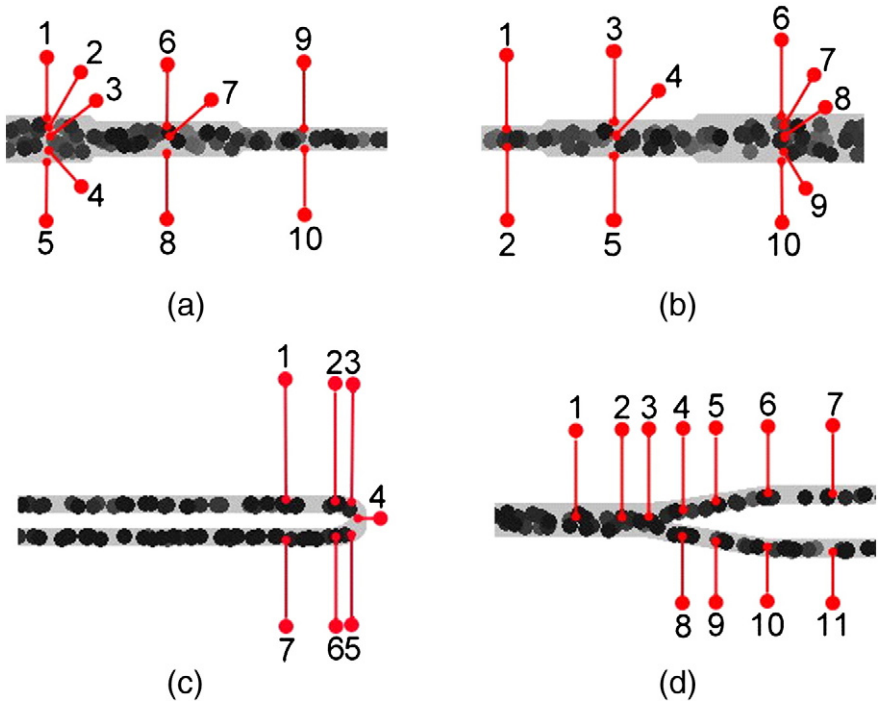

Fig. 5. The measurement position in various cases of micro-vessel bed.

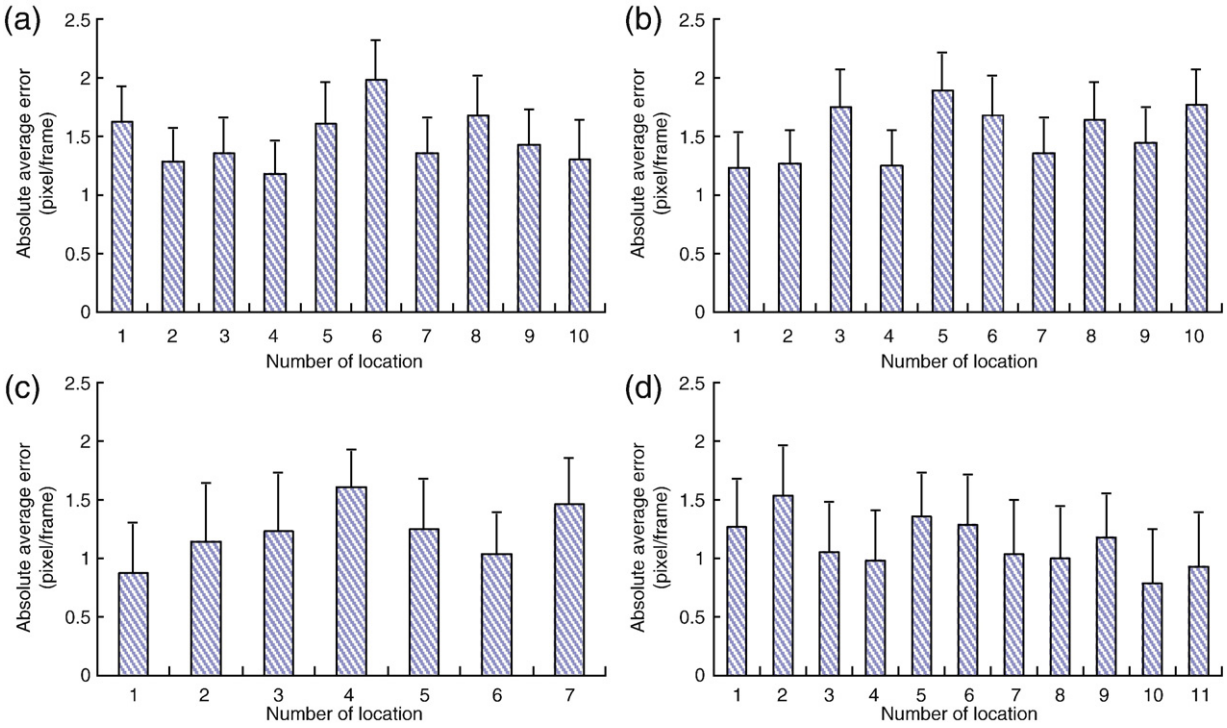

Fig. 6. The velocity analysis using OFM in micro-vessels at selected points.

maximal velocity of 1, 3, and 5 pixels, respectively. The worst relative error occurred at the highest maximum velocity case (10 pixels/frame), while the worst relative average error was at the lowest maximum velocity case (1 pixel/frame). The relative average error can be as high as 25% (Fig. 7b).

Conclusions

Three methods, which are commonly applied in red blood cell (RBC) velocity measurement in micro-vessels, were evaluated with simulated microscopic video image sequences in this study. The optical flow method (OFM) demonstrated superior accuracy over the cross-correlation method (CCM) and Hough transform method (HTM). With larger size vessels, for which both CCM and HTM have difficulties in RBC velocity estimation, OFM can still provide accurate results. This comparison study concluded that OFM is suitable for

Table 2
The absolute average error by suing OFM in different RBC densities with the same micro-vessel bed.

The average error estimation of RBC velocity, Mean ± S.D. (pixel/frame)				
	RBC movement, maximum (average)			
Velocity	1 pixel	3 pixels	5 pixels	10 pixels
Density	(0.7)	(2.1)	(3.5)	(7)
Low	0.200 ± 0.157	0.220 ± 0.176	0.267 ± 0.171	2.107 ± 0.776
Medium	0.203 ± 0.159	0.235 ± 0.171	0.268 ± 0.168	1.440 ± 0.578
High	0.204 ± 0.172	0.246 ± 0.175	0.281 ± 0.177	0.911 ± 0.473
Overall	0.202 ± 0.163	0.234 ± 0.174	0.272 ± 0.172	1.486 ± 0.609

Table 3
The relative average errors by suing OFM in different RBC densities with the same micro-vessel bed.

The percentage of average error in different RBCs velocity (%)				
	Maximal velocity			
Velocity	1 pixel	3 pixels	5 pixels	10 pixels
Density				
Low	28.6	10.5	7.6	30.1
Medium	29.0	11.2	7.7	20.6
High	29.1	11.7	8.0	13.0
Overall Mean ± S.D. (C.V.)	28.9 ± 0.3 (0.9)	11.1 ± 0.6 (5.4)	7.8 ± 0.2 (2.7)	21.2 ± 8.6 (40.3)

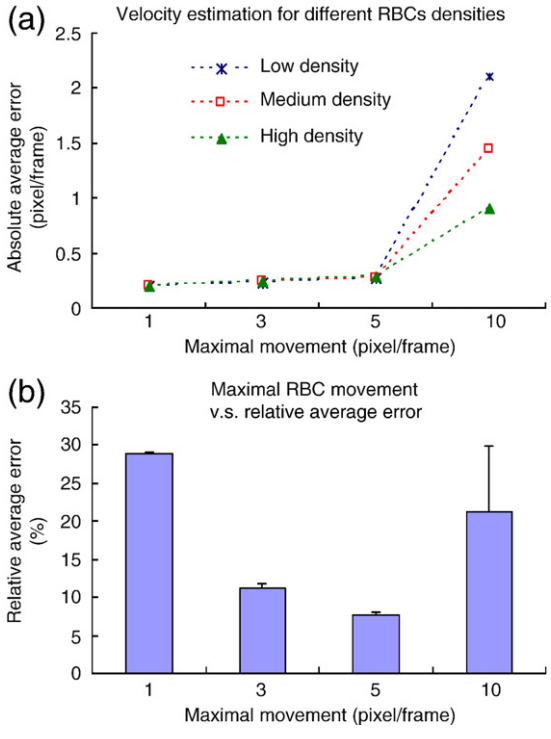

Fig. 7. The velocity estimation in various RBCs densities within same micro-vessel: (a) absolute average errors, (b) relative average errors.

accurate measurement of the RBC velocity in small or large micro-vessels.

In the future work, OFM will be applied to estimate the blood flow velocity in micro-vessels in vivo laboratory animals to analyze the change of blood flow velocity on the surface of tumor as tumor grows.

Acknowledgment

This study was financially supported by the school project of China Medical University, Taiwan (CMU-98-C-10).

References

Bertuglia, S., Leger, P., Colantuoni, A., Coppini, G., Bendayan, P., Boccalon, H., 1999. Different flowmotion patterns inhealthy controls and patients with Raynaud's phenomenon Technol. Health Care 7, 113–123.

Bollinger, A., Butti, P., Barras, J.P., Trachsler, H., Siegenthaler, W., 1974. Red blood cell velocity in nailfold capillaries of man measured by a television microscopy technique. Microvasc. Res. 7, 62–72.

Bonacci, E., Santacroce, N., D'Amico, N., Mattace, R., 1996. Nail-fold capillaroscopy in the study of microcirculation in elderly hypertensive patients. Arch. Gerontol. Geriatr. suppl. 5, 79–83.

Brox, T., Weickert, J., 2002. Nonlinear matrix diffusion for optic flow estimation 24th DAGM Symp: Springer LNCS, vol. 2449, pp. 446–453.

Cesarone, M.R., Incandela, L., Ledda, A., De Sanctis, M.T., Steigerwalt, R., Pellegrini, L., Bucci, M., Belcaro, G., Ciccarelli, R., 2000. Pressure and microcirculatory effects of treatment with lercanidipine in hypertensive patients and invascular patients with hypertension. Angiology 51, 53–63.

Chang, Chung-Hsing, Tsai, Rong-Kung, Wu, Wen-Chuan, Kuo, Song-Ling, Yu, Hsin-Su, 1997. Use of dynamic capillaroscopy for studying cutaneous microcirculation in patients with diabetes mellitus. Microvasc. Res. 53, 121–127.

Dobbe, J.G.G., Streekstra, G.J., Atasever, B., van Zijderveld, R., Ince, C., 2008. Measurement of functional microcirculatory geometry and velocity distributions using automated image analysis. Med. Biol. Eng. Comput. 46, 659–670.

Guerrero, T., Zhang, G., Huang, T.-C., et al., 2004. Intrathoracic tumour motion estimation from CT imaging using the 3D optical flow method. Phys. Med. Biol. 49, 4147–4161.

Horn, B.K.P., Schunck, B.G., 1981. Determining optical flow. Artif. Intell. 17, 185–203.

Huang, T., Zhang, G., Guerrero, T., et al., 2006. Semi-automated CT segmentation using optic flow and Fourier interpolation techniques. Comput. Methods Progr. Biomed. 84, 124–134.

Kempczynski, A., Grzegorzewski, B., 2008. Estimation of red blood cell aggregate velocity during sedimentation using the Hough transform. Opt. Commun. 281, 5487–5491.

Manjunatha, M., Singh, M., 2002. Computerised visualisation from images of blood flow through frog mesenteric microvessels with multiple complexities. Med. Biol. Eng. Comput. 40, 634–640.

Sugii, Y., Nishio, S., Okamoto, K., 2002. In vivo PIV measurement of red blood cell velocity field in microvessels considering mesentery motion. Physiol. Meas. 23 (2), 403–416.

Tibiriçá, E., Rodrigues, E., Cobas, R.A., Gomes, M.B., 2007. Endothelial function in patients with type 1 diabetes evaluated by skin capillary recruitment. Microvasc. Res. 73, 107–112.

Tsukada, K., Minamitani, H., Sekizuka, E., Oshio, C., 2000. Image correlation method for measuring blood flow velocity in microcirculation: correlation 'window' simulation and in vivo image analysis. Physiological Measurement 21 (4), 459–471.

Wollersheim, H., Reyenga, J., Thien, T., 1988. Laser Doppler velocimetry of fingertips during heat provocation in normals and in patients with Raynaud's phenomenon Scand. J. Clin. Lab. Invest. 48, 91–95.

Wu, Chih-Chieh, Zhang, Geoffrey, Huangc, Tzung-Chi, Lin, Kang-Ping, 2009. Red blood cell velocity measurements of complete capillary in finger nail-fold using optical flow estimation. Microvasc. Res. 78, 63–68.

Zhang, G., Huang, T.-C., Forster, K., et al., 2008a. Dose mapping: validation in 4D dosimetry with measurements and application in radiotherapy follow-up evaluation. Comput. Methods Progr. Biomed. 90, 25–37.

Zhang, G., Huang, T.-C., Guerrero, T., et al., 2008b. Use of three-dimensional (3D) optical flow method in mapping 3D anatomic structure and tumor contours across four-dimensional computed tomography data. J. Appl. Clin. Med. Phys. 9, 59–69.